Hindawi Publishing Corporation
Advances in Power Electronics
Volume 2012, Article ID 604703, 8 pages
doi:10.1155/2012/604703

Research Article

Implementation and Control of an AC/DC/AC Converter for Double Wound Flywheel Application

J. G. Oliveira,[1] H. Schettino,[2] V. Gama,[2] R. Carvalho,[2] and H. Bernhoff[1]

[1] *Division for Electricity, Uppsala University, 751 05 Uppsala, Sweden*
[2] *Electrical Engineering Department, Federal University of Juiz de Fora, 36036-900 Juiz de Fora, MG, Brazil*

Correspondence should be addressed to J. G. Oliveira, janaina.goncalves@angstrom.uu.se

Received 23 December 2011; Accepted 22 March 2012

Academic Editor: Henry S. H. Chung

An all-electric driveline based on a double wound flywheel, connected in series between main energy storage and a wheel motor, is presented. The flywheel works as a power buffer, allowing the battery to deliver optimized power. It also separates electrically the system in two sides, with the battery connected to the low voltage side and the wheel motor connected to the high voltage side. This paper presents the implementation and control of the AC/DC/AC converter, used to connect the flywheel high voltage windings to the wheel motor. The converter general operation and the adopted control strategy are discussed. The implementation of the AC/DC/AC converter has been described from a practical perspective. Results from experimental tests performed in the full-system prototype are presented. The prototype system is running with satisfactory stability during acceleration mode. Good efficiency and unity power factor could be achieved, based on vector control and space vector modulation.

1. Introduction

Extensive research has been recently done on Electric Vehicles (EVs) [1, 2]. The development of an efficient and robust propulsion system is essential to the feasibility of EVs [3]. But, even though sophisticated engines and advanced electrical power trains exist, the main issue, the long-term energy storage, has not been resolved.

All-electric drivelines based on battery, supercapacitor, flywheel, and combinations of these are being widely discussed and tested, attempting to lower the requirement on power density from the batteries [4, 5].

The propulsion system in development at Uppsala University is based upon a double wound flywheel energy storage device [6]. The flywheel under study is physically divided into two voltage levels through the stator winding. The high voltage side of the flywheel is connected to the wheel motor, whereas the low voltage side is connected to the battery, as shown in Figure 1. The system is bidirectional and the power can either flow from the battery to the wheel motor (acceleration mode) or from the wheel-motor to the battery (regenerative braking) [7].

In acceleration mode, the flywheel function is basically to provide the variant power requested by the wheel motor, so that the battery delivers a smoother output power. In braking mode, the wheel motor acts as a generator, and the flywheel is responsible for storing the regenerated energy.

The system needs a considerable number of power electronics converters and electronic controllers in order to regulate and optimize the power flux between the components [8]. A DC/AC converter is used to connect the battery to the flywheel low voltage side. An AC/DC/AC converter is used to connect the flywheel high voltage side to the wheel motor.

This paper presents the implementation and control of the AC/DC/AC converter to link the flywheel high voltage side to the wheel motor. Although it is a bidirectional converter, only the acceleration mode is studied in the present paper. Section 2 describes the modeling and general operation of the converter. The adopted control strategy

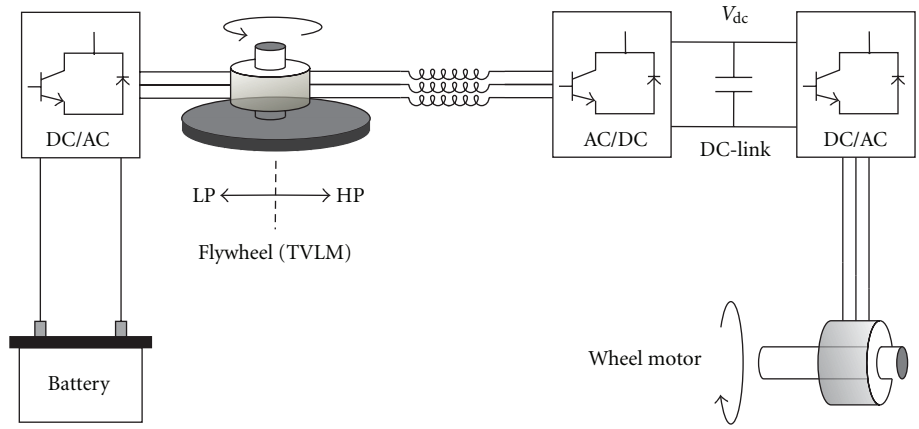

Figure 1: All-electric driveline schematics: The power can flow in both directions.

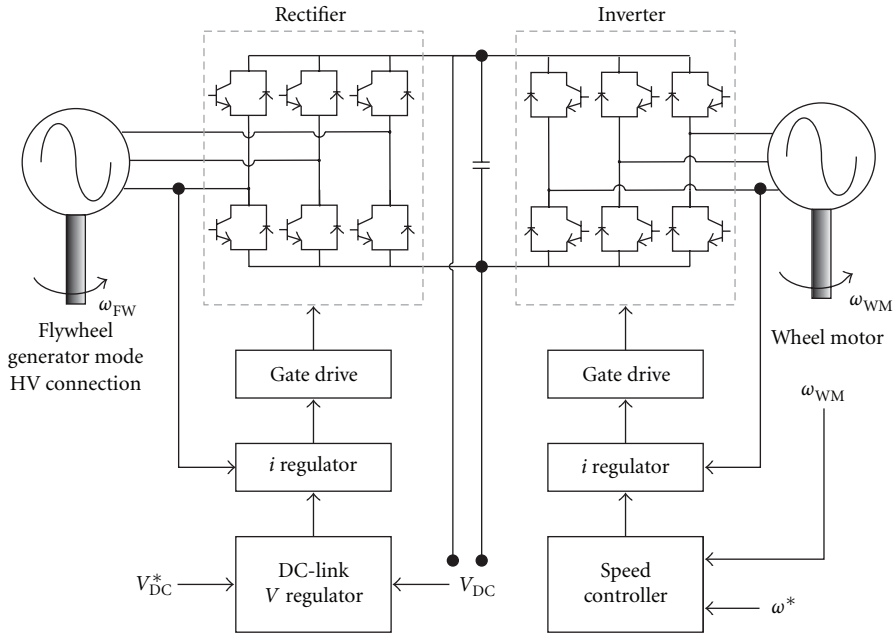

Figure 2: The AC/DC/AC converter in acceleration mode.

is discussed in details in Section 3. A prototype system is presented in Section 4, and the experimental results are discussed in Section 5.

2. The AC/DC/AC Converter

Both the wheel motor and the flywheel machine are three-phase synchronous machines in the present system. The angular speed of synchronous machines is proportional to the applied electric frequency in steady state. The energy stored in the flywheel rotor is related to its angular speed. The wheel motor speed must vary according to the vehicle's requirements.

The AC/DC/AC converter is an electrical way to decouple the two frequencies. Two identical three-phase bridges, one capacitor and inductors compose the power circuit. In acceleration mode, the AC/DC/AC converter can be divided into a rectifier and an inverter, as shown Figure 2. This section presents briefly the modeling and functioning of the two modules.

2.1. Rectifier. A forced-commutated three-phase controlled rectifier is required to obtain a desired voltage in the DC-link for different flywheel speeds and different wheel motor loads [9]. A scheme of the forced-commutated rectifier, based on transistors, is shown in Figure 2.

The AC/DC converter must behave like a voltage boost in order to work as a forced-commutated rectifier. In other words, the DC-Link voltage must be larger than the peak DC voltage generated by the rectifying diodes in passive mode. The inductance L performs the boost voltage operation in combination with the capacitor C and acts at the same time as a low-pass filter for the AC line current. Therefore, the choice of L and C values is extremely important for the

proper functioning of the rectifier. Since the flywheel has a very small internal inductance, external inductors need to be placed.

Assuming that the source (flywheel machine) is a balanced, sinusoidal three-phase voltage supply with frequency ω, the input voltages can be written as

$$\begin{aligned} e_a &= -E\sin(\omega t), \\ e_b &= -E\sin\left(\omega t - \frac{2\pi}{3}\right), \\ e_c &= -E\sin\left(\omega t + \frac{2\pi}{3}\right). \end{aligned} \tag{1}$$

In the rotating d-q frame, the input voltage is usually in the quadrature axis [10]. Therefore, the direct component is null

$$\begin{aligned} e_d &= 0, \\ e_q &= E. \end{aligned} \tag{2}$$

The voltage equation in the rotating d-q frame is given by

$$\begin{aligned} 0 &= L\frac{di_d}{dt} - \omega L i_q + V_d, \\ E &= L\frac{di_q}{dt} + \omega L i_d + V_q. \end{aligned} \tag{3}$$

The active power supplied from the source is

$$P = \frac{3}{2}\left(e_q i_q + e_d i_d\right) = \frac{3}{2}E i_q. \tag{4}$$

If the i_d current is controlled to zero, the line current is completely represented by i_q component and the active power coming from the source is maximized. Consequently, the input current will be in phase with the input voltage (unity power factor)

$$i_d^* = 0. \tag{5}$$

The idea of the proposed control strategy is to control the DC voltage in combination with the input AC currents so that unity power factor is reached. Instantaneous value of the DC voltage, input currents, and flywheel speed must be known to achieve closed loop control. The control strategy adopted is discussed in detail in Section 3.

2.2. Inverter. The inverter is responsible for driving the wheel motor, controlling its angular speed for different load torques. Since the wheel motor is a synchronous permanent magnetic machine (PMSM), the electromagnetic torque expressed in the d-q rotating frame is given by [11]

$$T_e = \frac{3p}{2}\left[\psi_{\mathrm{PM}} i_q + i_q i_d\left(L_d - L_q\right)\right], \tag{6}$$

where p is the number of pole pairs; ψ_{PM} is the flux produced by the permanent magnet; L_d and L_q are, respectively, the direct and quadrature components of the wheel motor inductance.

Considering a nonsalient pole machine (smooth air gap), L_d and L_q are the same, and (5) can be written as

$$T_e = \frac{3p}{2}\psi_{\mathrm{PM}} i_q = K i_q. \tag{7}$$

According to (7), only the i_q component can influence the value of the electromagnetic torque produced in the machine. Thus, the maximum torque per ampere occurs when i_q is at its maximum value and, consequently, i_d is equal to zero

$$i_d^* = 0. \tag{8}$$

The implementation of the inverter control requires the feedback signals of the line currents and rotor position instantaneous values, as shown Figure 4. The details of the control strategy are further explained in Section 3.

3. Control Strategy

3.1. DC-Link Control. A simplified diagram of the DC-link control is shown in Figure 3. Due to the characteristic of closed loop, it is necessary to measure the stator currents and rotor angular position. These measurements are carried out by two current sensors, and a hall sensor used to calculate the speed and estimate the rotor position. The instantaneous values of stator currents i_a and i_b are mathematically transformed (Clarke and Park transformations) and then used as the feedback for i_q and i_d control loops.

An outer loop of voltage is connected to a PID regulator. The output of the voltage controller is the reference of the quadrature current i_q. The reference of the direct current i_d is set to zero, in order to obtain unity power factor operation. The output of i_q and i_d PID controllers are transformed into α and β components (Inv Park) and modulated by Space Vector modulation, generating the pulses that are inserted into a three-phase bridge rectifier.

3.2. Vector Control. The Vector control block diagram is similar to the DC-Link diagram, as shown in Figure 4. Current sensors are necessary to capture the instantaneous values of the line currents. In this case, an encoder was used to measure the rotor angular position. The two inner currents loops are maintained in exactly the same way as for the DC-link control. The main difference is in the outer loop, where a speed loop control is implemented. The output of the speed controller is the reference quadrature current i_q, which regulates the torque needed to reach the reference speed. The reference of the direct current i_d is set to zero, in order to obtain maximum torque per ampere in the machine.

4. Prototype System

A scaled experimental test setup has been constructed to investigate the properties of the proposed flywheel system [12]. The experiment allows measurements of complete drive cycles to be performed, improving the understanding of the constituting components and optimization of the complete system.

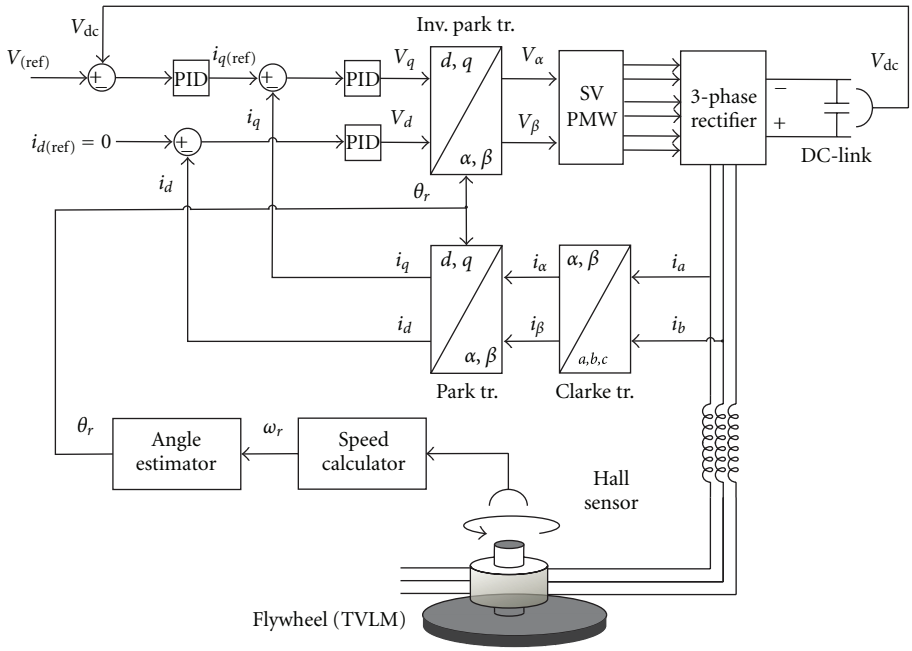

Figure 3: Block diagram of the DC-Link control.

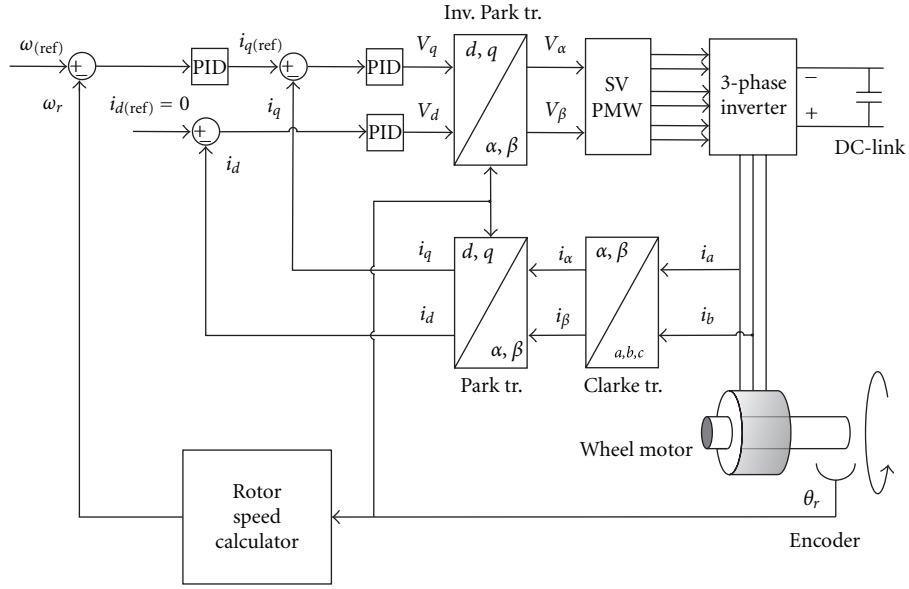

Figure 4: Block diagram of the Vector control.

A prototype of the described AC/DC/AC converter that connects the high voltage of the flywheel machine to the wheel motor has been implemented.

A 3.5 kW/380 V PMSM (manufacturer *Leroy Somer*) is used as wheel motor. The double wound flywheel machine is a prototype developed at Uppsala University [6]. A DC power supply emulates a battery, connected through a DC/AC converter to the low-voltage side of the flywheel (not shown in the diagram).

The high-voltage side of the flywheel is connected to 600 μH inductors per phase, required for the functionality of the forced-commutated rectifier. A 20 mF/350 V capacitor is connected in parallel with the DC-Link.

Two three-phase *MOSFET* bridges were built with discrete *DSEI 2130*. A *snubber* circuit was implemented in order to eliminate the rings presented in the *MOSFET* output.

The control of the AC/DC/AC converter has been performed using two MCUs (Microcontrollers) Piccolo

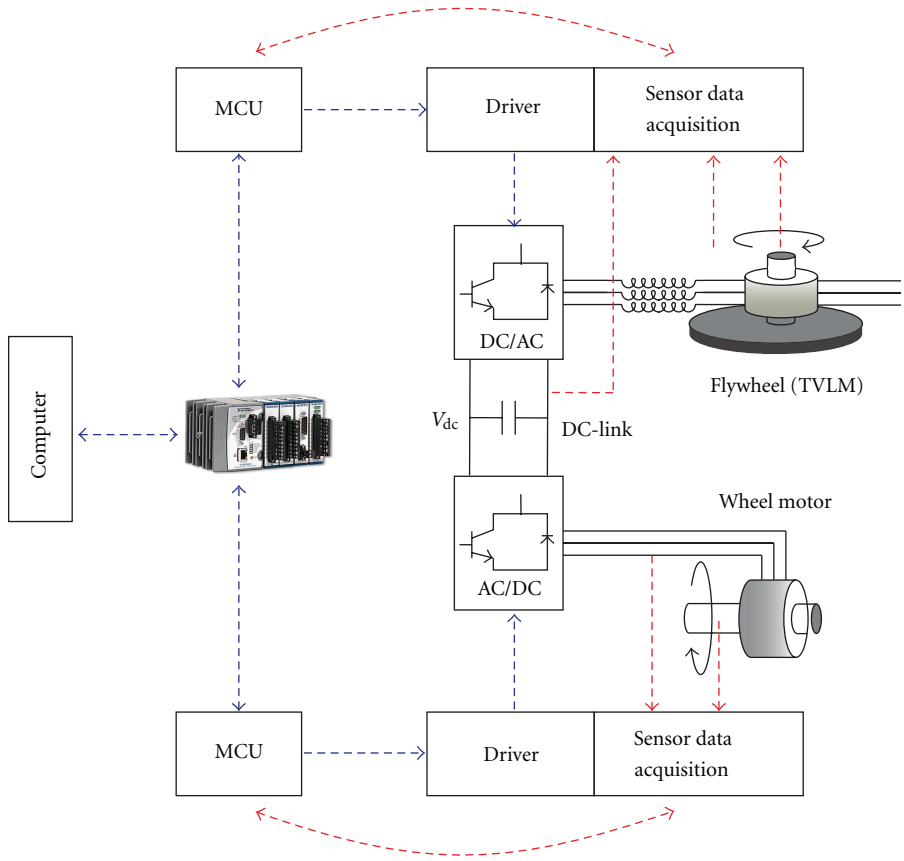

Figure 5: Prototype System, the black arrows indicate the sensor signals flux.

TMDSCNCD28035 (manufactured by Texas Instruments) plugged in the TMDSDOCK28035 Experimenter's Kit.

The current setup has two MCU and one computer, which perform real-time debug, through serial communication using a Compact Rio device from National Instruments, as shown in Figure 5.

Two mainboards, one for each module of the converter, contain the driver and sensor circuits. The driver used is an IR2130, from *International Rectifier*. With the purpose of avoiding damage in the low power system, the driver was electrically isolated from the MCU by digital optocouplers (A4800). The system requires a large number of sensors: four current sensors (HAL50-S), one encoder (ERN423), one voltage sensor (resistive divider), and three hall sensors (A1101). The current sensors are used in both boards to capture the instantaneous values of the line AC currents. The hall sensor (flywheel speed capture) and the voltage sensor (DC-Link voltage capture) are used for the rectifier control strategy. The encoder is used to estimate the wheel motor rotor angle for the inverter board. The black arrows in Figure 5 indicate the sensor signals flux.

The rectifier main board with the components indications is shown in Figure 6. Small changes are seen in the inverter mainboard due to the different sensors used.

5. Experimental Results

The experimental waveforms for a 20-second test performed in the full system prototype are shown in Figure 7, Figure 8, and Figure 9. A variant torque is applied to the wheel motor up to $t = 11$ s, as seen in Figure 7.

The approximate input and output power curves can be seen in Figure 8. The mean input power, measured in the terminals of the DC power supply, is 140 W and the mean output power, measured from voltage and current supplied to the wheel motor, is 125 W.

The flywheel speed decreases from 1950 RPM to 1650 RPM in order to supply the power requested by the wheel motor, as seen in Figure 9. When the torque is changed to a small constant value ($t > 11$ s), the flywheel speed increases to the initial value (1950 RPM). While the torque is being applied, a stationary error of about 10% compared to the setpoint values occurs in the motor speed control (Figure 9).

Additional experimental results are shown in Figures 10, 11, and 12.

Different load current and different reference values for the DC-link voltage were applied to the system in order to verify the controllers' response. The rotational speed of

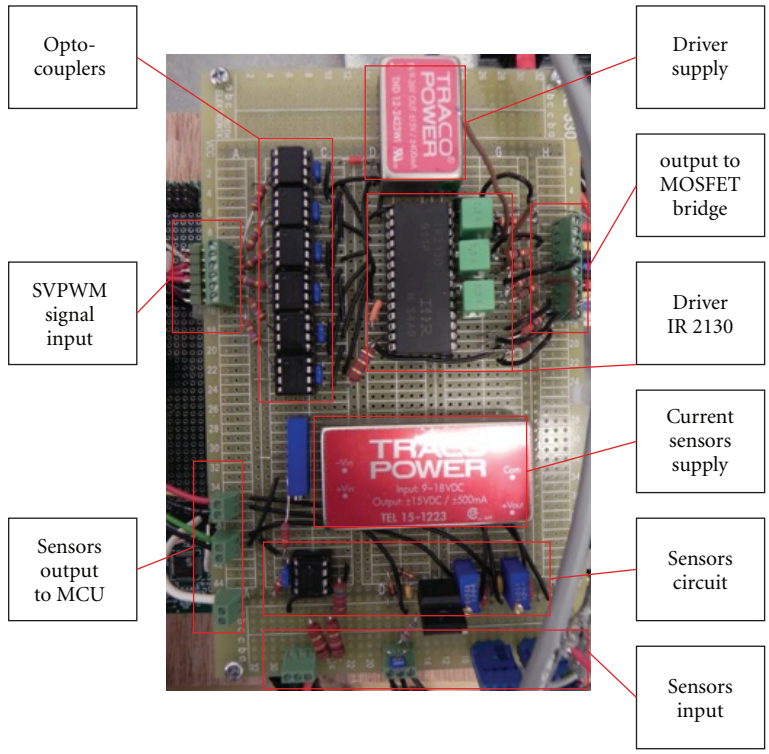

Figure 6: Rectifier main circuit board.

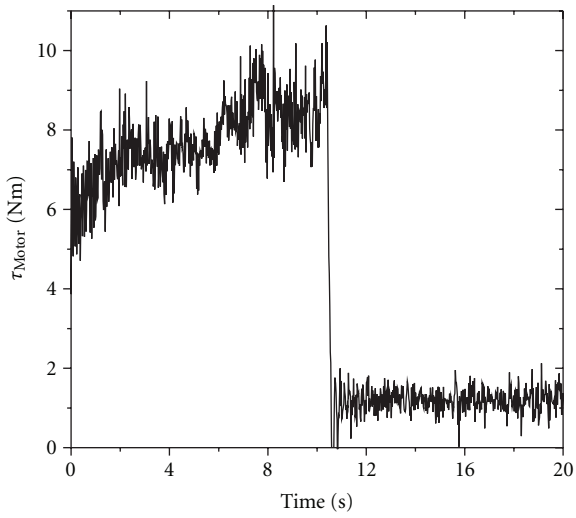

Figure 7: Applied torque.

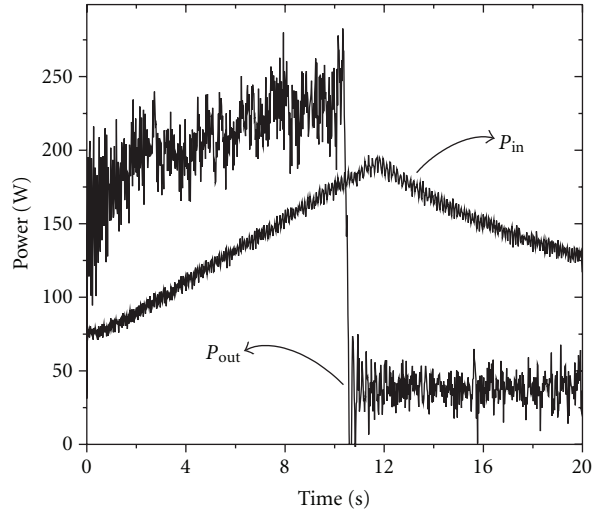

Figure 8: Input and output power.

the flywheel machine varies in order to supply the extra current required on the motor side, as shown in Figure 10(a). Different output currents are shown in Figure 10(b). The voltage on the DC-link is kept constant, with some oscillations when the applied load is changed. Small overshoot can be seen when the reference value was changed. These oscillations might indicate that the PID parameters can be further adjusted.

The flywheel was disconnected from the battery, and the load was kept the same, so the output current of the DC-link would not vary. The speed of the flywheel decreased as shown in Figure 11(a). The voltage in the DC-link was kept constant (80 V) until the speed the flywheel was around 20 rpm, as shown in Figure 11(b). The output current on the flywheel high power side is shown in Figure 11(c). It increased as the speed of the flywheel decreased, to compensate for the falling output voltage.

Output voltage and current on the high voltage of the flywheel machine for different reference values of I_d is shown in Figure 12. As described in Section 2, unity power factor

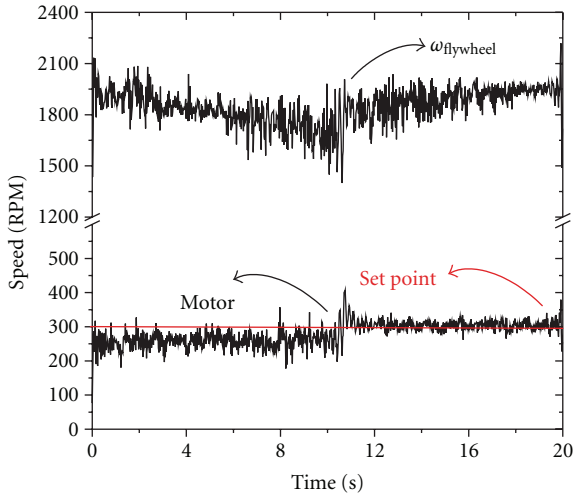

Figure 9: Flywheel and wheel motor angular speed.

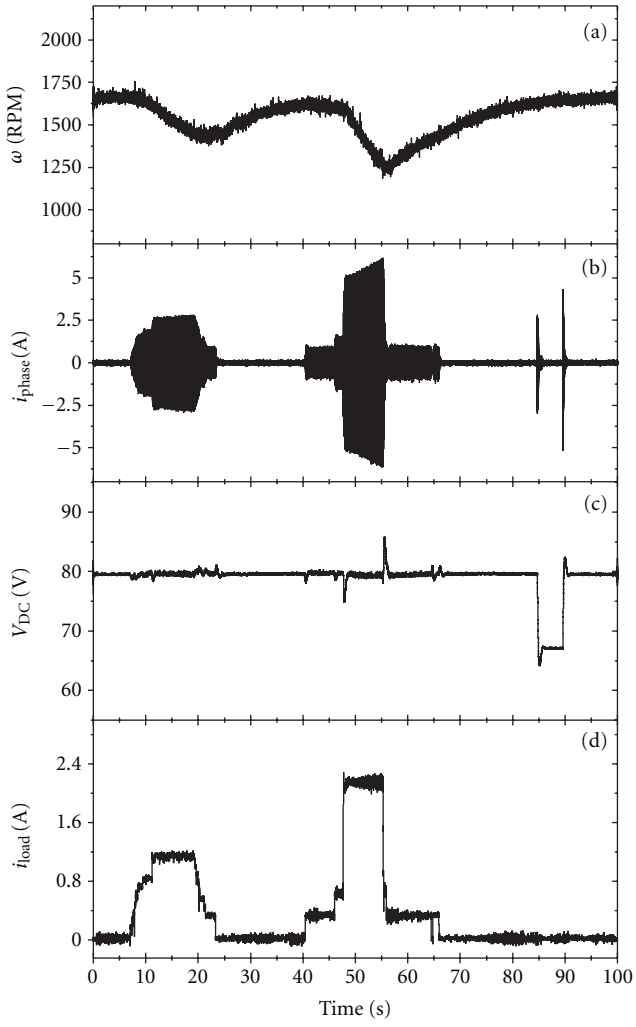

Figure 10: (a) Speed of the flywheel, (b) flywheel output current, (c) DC-link voltage, and (d) wheel motor current.

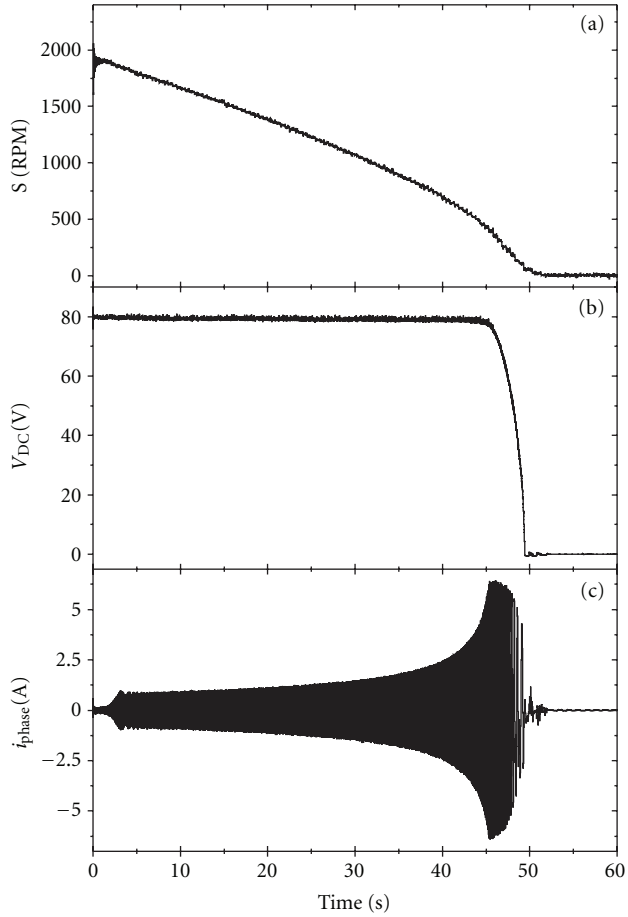

Figure 11: (a) Speed of the flywheel, (b) voltage over the DC link, and (c) flywheel output current.

operation is desired on the rectifier side, and this is achieved by making $I_d = 0$ in nonsalient pole machines. The results shown in Figure 12 indicate that the flywheel machine is not purely nonsalient, and due to some small saliency, the required value of I_d in order to reach unity power operation is different from zero (the values are given in p.u. in Figure 12).

6. Conclusion

An AC/DC/AC converter based on MOSFET modules for double wound flywheel application is presented. The prototype system is running with satisfactory stability in acceleration mode. Some changes in the control system must be implemented in order to achieve regenerative braking. Based on vector control theory and space vector modulation, good efficiency and unity power factor could be achieved.

Results have shown some oscillations in the control of the DC-link voltage, which can be suppressed with further adjustment of the PID parameters. However, the control has shown robustness and capability of keeping the DC-link voltage constant for a broad range of input voltages.

Small saliency of the flywheel machine has been shown by the results, but unity power factor operation can be reached by slightly adjusting the value of I_d in the control system.

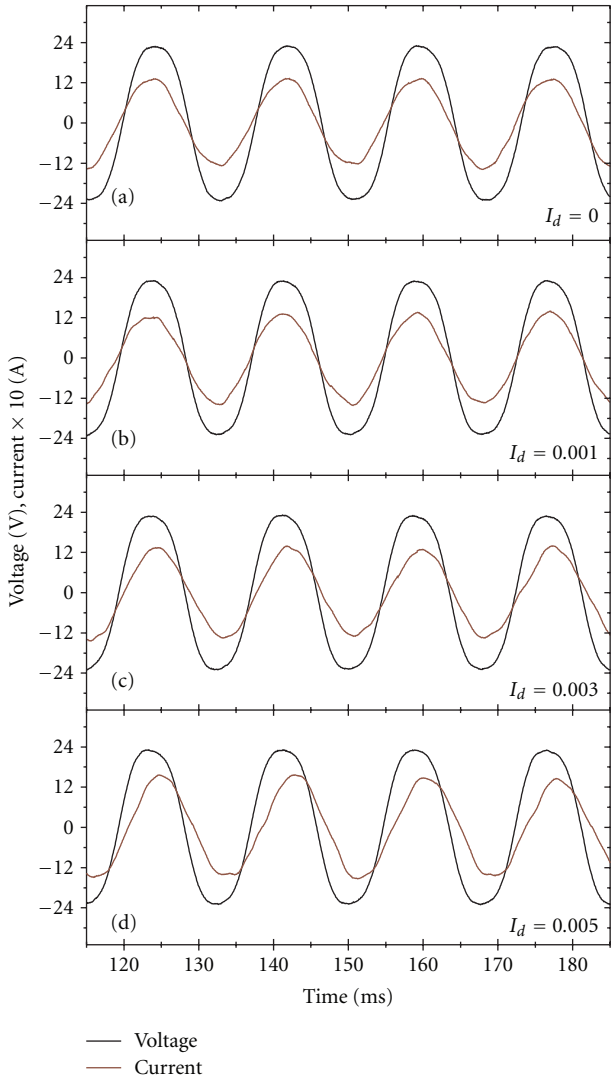

Figure 12: Output voltage and current on the high voltage of the flywheel machine for different reference values of I_d.

Future work consists in implementing regenerative braking operation and enlarging the system to a full-scale experimental setup.

Acknowledgments

The authors would like to thank Dr. Juan de Santiago, Licentiate Johan Abrahamsson and Licentiate Johan Lundin for their contribution to this work. Also to Professor Francisco José Gomes and PET/MEC, from the Federal University of Juiz de Fora.

References

[1] J. Dixon, "Energy storage for electric vehicles," in *Proceedings of the IEEE-ICIT International Conference on Industrial Technology (ICIT '10)*, pp. 20–25, March 2010.

[2] P. Fairley, "Speed bumps ahead for electric-vehicle charging," *IEEE Spectrum*, vol. 47, no. 1, pp. 13–14, 2010.

[3] A. Emadi, S. S. Williamson, and A. Khaligh, "Power electronics intensive solutions for advanced electric, hybrid electric, and fuel cell vehicular power systems," *IEEE Transactions on Power Electronics*, vol. 21, no. 3, pp. 567–577, 2006.

[4] J. Van Mierlo, P. Van den Bossche, and G. Maggetto, "Models of energy sources for EV and HEV: fuel cells, batteries, ultracapacitors, flywheels and engine-generators," *Journal of Power Sources*, vol. 128, no. 1, pp. 76–89, 2004.

[5] J. Santiago, J. G. Oliveira, J. Lundin, J. Abrahamsson, A. Larsson, and H. Bernhoff, "Design parameters calculation of a novel driveline for electric vehicles," *World Electric Vehicle Journal*, vol. 3, 2009.

[6] J. De Santiago, A. Larsson, and H. Bernhoff, "Dual voltage driveline for vehicle applications," *International Journal of Emerging Electric Power Systems*, vol. 11, no. 3, article 1, 2010.

[7] J. G. De Oliveira, J. Lundin, J. De Santiago, and H. Bernhoff, "A double wound flywheel system under standard drive cycles: simulations and experiments," *International Journal of Emerging Electric Power Systems*, vol. 11, no. 4, article 6, 2010.

[8] J. G. Oliveira and H. Bernhoff, "Power electronics and control of two-voltage-level flywheel based all-electric driveline," in *IEEE International Symposium on Industrial Electronics*, 2011.

[9] M. H. Rashid, *Power Electronics Handbook*, Academic Press, 2001.

[10] J. W. Choi and S. K. Sul, "Fast current controller in 3-phase AC/DC boost converter using d-q axis cross-coupling," in *Proceedings of the 27th Annual IEEE Power Electronics Specialists Conference (PESC '96)*, vol. 1, pp. 177–182, January 1996.

[11] K. S. Low, M. F. Rahman, and K. W. Lim, "Dq transformation and feedback linearization of a permanent magnet synchronous motor," in *Proceedings of the International Conference on Power Electronics and Drive Systems*, pp. 292–296, February 1995.

[12] J. Abrahamsson, J. De Santiago, J. G. Oliveira, J. Lundin, and H. Bernhoff, "Prototype of electric driveline with magnetically levitated double wound motor," in *Proceedings of the 19th International Conference on Electrical Machines (ICEM '10)*, September 2010.